

Article

# Neutrino Physics and Astrophysics with the JUNO Detector

Lino Miramonti <sup>1,\*</sup>  on behalf of the JUNO Collaboration

<sup>1</sup> Dipartimento di Fisica, Università degli Studi di Milano and I.N.F.N. Sezione di Milano, Via Celoria 16, 20133-Milano (Italy); lino.miramonti@mi.infn.it

\* Correspondence: lino.miramonti@mi.infn.it; Tel.: +39-025031304

**Abstract:** The Jiangmen Underground Neutrino Observatory (JUNO) is a 20 kton liquid scintillator multi-purpose underground detector, under construction near the chinese city of Jiangmen, with data taking expected to start in 2021. The main goal of the experiment is the neutrino mass hierarchy determination, with more than three sigma significance, and the high precision neutrino oscillation parameters measurements, detecting electron anti-neutrinos, emitted from two near-by (baseline of about 53 km) nuclear power plants. Besides, the unprecedented liquid scintillator type detector performance in target mass, energy resolution, energy calibration precision and low-energy threshold, features a rich physics program for the detection of low-energy astrophysical neutrinos, such as galactic core-collapse supernova neutrinos, solar neutrinos and geo-neutrinos.

**Keywords:** JUNO; liquid scintillator; neutrino mass hierarchy.

## 1. Introduction, how to infer the mass hierarchy

Among the remaining undetermined fundamental aspects in the leptonic sector of Standard Model, there is the neutrino mass hierarchy determination; i.e. whether the  $\nu_3$  neutrino mass eigenstate is heavier or lighter than the  $\nu_1$  and  $\nu_2$  mass eigenstates. The mass hierarchy discrimination will have an impact in neutrino nature quest (Dirac or Majorana) [1]. The two possible scenarios, still compatible with the huge amount of data from different classes of neutrino experiments, usually denoted as normal and inverse hierarchy (NH and IH), are represented in fig.1. Denoting the squared mass eigenvalues differences as  $\Delta m_{ij}^2 = m_i^2 - m_j^2$ , in normal hierarchy case the third neutrino mass eigenvalue would be the biggest one and  $|\Delta m_{31}^2| = |\Delta m_{32}^2| + \Delta m_{21}^2$ . Instead in inverted hierarchy case,  $m_3$  would be the smallest eigenvalue and the relation would be  $|\Delta m_{31}^2| = |\Delta m_{32}^2| - \Delta m_{21}^2$ . According to the most recent global analyses, the squared mass differences are<sup>1</sup>:

$$\Delta m_{21}^2 = (7.37 \pm 0.17) \times 10^{-5} \text{eV}^2; \quad (1)$$

$$|\Delta m_{32}^2| = (2.52 \pm 0.04) \times 10^{-3} \text{eV}^2. \quad (2)$$

The relative high value of the  $\theta_{13}$  angle, ( $\theta_{13} = 8.46_{-15}^{+15}$ , at  $1\sigma$  for the normal hierarchy [3]) makes possible the realization of the idea [4] [5] to extract the mass hierarchy from the study of hierarchy dependent oscillation probability corrections, which are proportional to  $\sin^2\theta_{13}$ .

We can write the  $\bar{\nu}_e$  survival probability in the form:

<sup>1</sup> The first result is obtained mainly from solar neutrino and from KamLAND experiments- The second result is obtained mainly from atmospheric and by long baseline accelerator experiments. This second value would correspond to  $|\Delta m_{31}^2|$  in case of inverted hierarchy

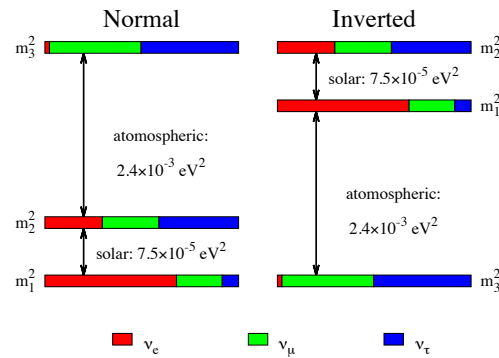


**Figure 1.** Neutrino mass eigenstate flavor composition and mass pattern in the two cases of normal (left) and inverted (right) hierarchies. Taken from [2].

$$\begin{aligned}
 P_{ee} &= 1 - \cos^4 \theta_{13} \sin^2 2\theta_{12} \sin^2 \frac{\Delta m_{21}^2 L}{4E} - \sin^2 2\theta_{13} \left( \cos^2 \theta_{12} \sin^2 \frac{\Delta m_{31}^2 L}{4E} + \sin^2 \theta_{12} \sin^2 \frac{\Delta m_{32}^2 L}{4E} \right) \\
 &= 1 - \cos^4 \theta_{13} \sin^2 2\theta_{12} \sin^2 \frac{\Delta m_{21}^2 L}{4E} - P_{MH}
 \end{aligned} \quad (3)$$

The last term of equation 3, indicated as  $P_{MH}$ , represents the mass hierarchy dependent contribution to the oscillation probability. It can be rewritten as:

$$P_{MH} = \frac{1}{2} \sin^2 2\theta_{13} \left( 1 - \sqrt{1 - \sin^2 2\theta_{12} \sin^2 \left( \frac{\Delta m_{21}^2 L}{4E} \right)} \cos \left( 2 \left| \frac{\Delta m_{ee}^2 L}{4E} \right| \pm \phi \right) \right), \quad (4)$$

where  $\Delta m_{ee}^2$  represents the combination  $\Delta m_{ee}^2 = (\cos^2 \theta_{12} \Delta m_{31}^2 + \sin^2 \theta_{12} \Delta m_{32}^2)$ . The new quantity  $\phi$  is defined in such a way that  $\sin \phi$  and  $\cos \phi$  are combinations of the mass and mixing parameters in the 1-2 sector<sup>2</sup>. The  $\pm$  sign, in the last term of equation 4, is decided by the MH, with plus sign for the normal one and minus sign for the inverted one. Hence the survival (or oscillation) probability and, consequently, the observed spectrum are characterized by the presence of fastly oscillating terms. Phases are in opposition for the two MH cases (NH and IH), superimposed to the general oscillation pattern valid for both hierarchies.

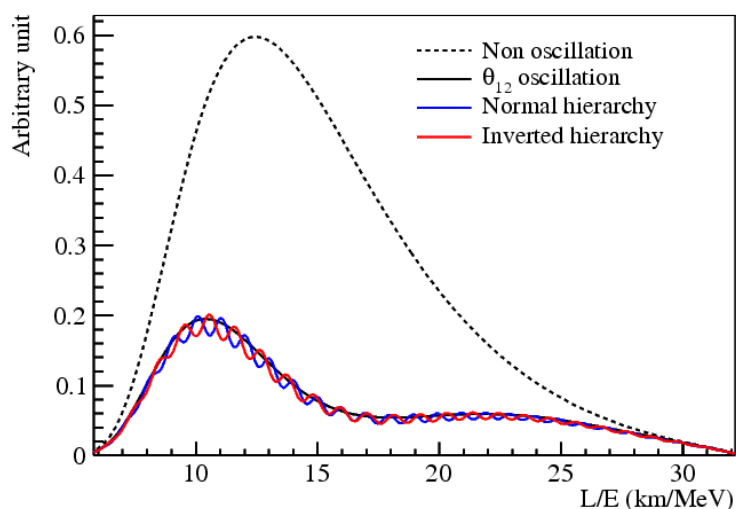
In order to discriminate between the two possible hierarchies, we need to determine the  $\nu$  energy spectrum with a very high energy resolution. The experimental signature of the reactor  $\bar{\nu}_e$  is given by the inverse beta decay process  $\bar{\nu}_e + p \rightarrow e^+ + n$ . The resulting signal is given by visible energy from the positron energy loss and annihilation, plus delayed light, at a fixed 2.2 MeV energy, from the neutron capture on protons.

Figure ?? shows the spectrum in non oscillating case (red line) and the expected spectrum for a detector with a baseline of about 50 km, as in JUNO experiment case. The hierarchy dependent corrections are in phase opposition; the blue line represent the NH and the green line the IH.

## 2. JUNO detector and capabilities

The JUNO (Jiangmen Underground Neutrino Observatory) detector will be built at a shallow depth, with an average overburden of about 700 m, close to Jiangmen City, in China, at a 53 km distance from the Yangjiang and Taishan nuclear power plants. The foreseen total power produced by the two facilities is about 26.6 GW.

<sup>2</sup> For the details of the calculation see [2]



**Figure 2.** The relative shape difference of the reactor antineutrino flux for different neutrino MHs. [2]

The core of the detector is composed by 20 kton of liquid scintillator (LS), contained in an acrylic sphere (12 cm thick, with an inner diameter of 35.4 m), kept in position by a stainless steel truss. This central detector is placed inside an active water pool that will act as a Cherenkov muon veto and will reduce gamma rays and neutrons coming from the rock. On top of the water pool there will be an external veto detector composed by plastic scintillators.

The LS is composed of LAB (Linear Alkyl Benzene) as solvent, with PPO (2.5-Diphenyloxazole) as fluor and bis-MSB, a wavelength shifter.

In order to attain the desired energy resolution to disentangle the two mass hierarchies, the JUNO Collaboration paid a particular attention to the photomultiplier system, that consists of 17000 large PMTs, with a diameter of 20 inches, interspersed with 25000 smaller ones, of 3 inches. This large number of PMTs will allow a powerful event reconstruction and will offer an internal cross check, that should help in reducing the non stochastic uncertainty and improving the high precision oscillation parameter measurement. The total coverage is about 80%, corresponding to about 1200 photo-electrons/MeV.

To analyze the spectrum, distinguishing the wiggles position and extracting the desired information on mass hierarchy, the total energy resolution must be  $\frac{\sigma_E}{\sqrt{E}} \leq 3\%$ .

### 3. Mass hierarchy and neutrino physics

The main goal of JUNO is to establish the neutrino mass hierarchy, by analyzing the spectrum of the antineutrino inverse  $\beta$  decay on proton. To obtain this result, the experimental spectrum will be compared with the theoretical one, which is a function of the oscillation parameters and of the mass hierarchy.

This discrimination is obtained by comparing the  $\chi^2$  values, corresponding to the two different hierarchies best fit points.

The term  $\Delta\chi_{MH}^2 = |\chi_{MIN}^2(NH) - \chi_{MIN}^2(IH)|$  is a measure of the *mass hierarchy sensitivity*, and represents the discrimination power of JUNO [2].

In addition to the mass hierarchy determination, JUNO will perform other measurements and analyses. Thanks to the very high statistics and the excellent energy resolution JUNO will provide a significant improvement in the precision measurement of the three masses and mixing parameters (see table 1) [3].

**Table 1.** Comparison of the present accuracy and the JUNO potentialities for 3 oscillation parameters

Oscillation parameter	Current accuracy (Global $1\sigma$ )	Dominant experiment(s)	JUNO potentialities
$\Delta m_{21}^2$	2.3%	KamLAND	0.59%
$\Delta m^2 = \left  m_3^2 - \frac{1}{2}(m_1^2 + m_2^2) \right $	1.6%	MINOS, T2K	0.44%
$\sin^2\theta_{12}$	$\sim 4 - 6\%$	SNO	0.67%

## 4. Neutrino astrophysics

### 4.1. Supernova neutrinos

The rich program of JUNO covers also neutrino astrophysics. A Supernova (SN) explosion causes the emission of a huge amount of energy in the form of neutrinos over a long time period. JUNO can perform studies of supernovas, both with the direct measurement of the neutrino burst produced by a nearby SN collapse and with the study of the diffuse supernova background (DSNB).

Analyzing the three different stages in which the SN explosion process can be divided: the very fast initial neutrino burst, the accretion and the cooling phases, it is possible to infer many parameters of interest for astrophysics and for elementary particle physics (see figure 3).

These three phases have a different emission spectrums, and thanks to this difference it is possible to obtain complementary information on the neutrino (antineutrino) flavor composition and luminosity.

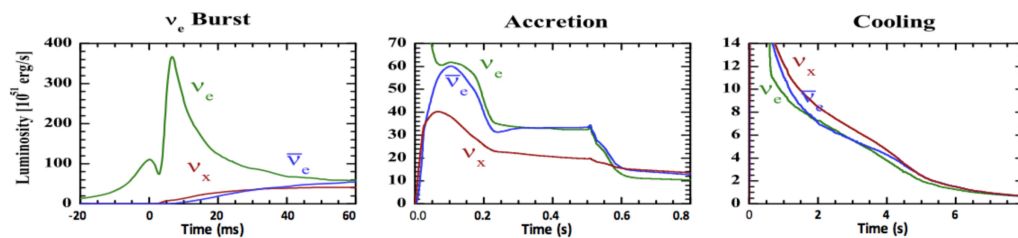


**Figure 3.** Three phases of neutrino emission from a core-collapse SN, from left to right: (1) Infall, bounce and initial shock-wave propagation, including prompt  $\nu_e$  burst. (2) Accretion phase with significant flavor differences of fluxes and spectra and time variations of the signal. (3) Cooling of the newly formed neutron star, only small flavor differences between fluxes and spectra. Figure from [2]

In the table 2 are reported the main interaction channels and the number of expected events, in JUNO, for a 10 kpc distant SN.

**Table 2.** Expected number of events in JUNO, for the main channels for neutrinos produced by a SN at a distance of 10 kpc. Taken from [2]

Process	Type	Events $\langle E_\nu \rangle = 14\text{MeV}$
$\bar{\nu}_e + p \rightarrow e^+ + n$	CC	$5.0 \times 10^3$
$\nu + p \rightarrow \nu + p$	NC	$1.2 \times 10^3$
$\nu + e^- \rightarrow \nu + e^-$	ES	$3.6 \times 10^2$
$\nu + {}^{12}\text{C} \rightarrow \nu + {}^{12}\text{C}^*$	NC	$3.2 \times 10^2$
$\nu_e + {}^{12}\text{C} \rightarrow e^- + {}^{12}\text{N}$	CC	$0.9 \times 10^2$
$\bar{\nu}_e + {}^{12}\text{C} \rightarrow e^+ + {}^{12}\text{B}$	CC	$1.1 \times 10^2$

### 4.2. Solar neutrinos

Also solar neutrinos can be studied with the JUNO detector. Despite the shallow site, the JUNO detector take advantage of its LS large mass, that guarantees a very high statistics, and of its very good energy resolution.

For these studies, a key parameter is the radiopurity level of the LS, in order to disentangle the signal from the different natural background sources. In particular the radioactive isotopes  $^{238}\text{U}$ ,  $^{232}\text{Th}$ ,  $^{40}\text{K}$ ,  $^{210}\text{Bi}$  and  $^{85}\text{Kr}$ . Table 3 shows the required background rate constrains, to conduct low energy solar neutrino measurements, and the estimated solar neutrino signal rates at JUNO.

**Table 3.** The requirements of singles background rates for doing low energy solar neutrino measurements and the estimated solar neutrino signal rates at JUNO. Taken from [2].

Internal radiopurity requirements		
	baseline	ideal
$^{210}\text{Pb}$	$5 \times 10^{-24}$ [g/g]	$1 \times 10^{-24}$ [g/g]
$^{85}\text{Kr}$	500 [counts/day/kton]	100 [counts/day/kton]
$^{238}\text{U}$	$1 \times 10^{-16}$ [g/g]	$1 \times 10^{-17}$ [g/g]
$^{232}\text{Th}$	$1 \times 10^{-16}$ [g/g]	$1 \times 10^{-17}$ [g/g]
$^{40}\text{K}$	$1 \times 10^{-17}$ [g/g]	$1 \times 10^{-18}$ [g/g]
$^{14}\text{C}$	$1 \times 10^{-17}$ [g/g]	$1 \times 10^{-18}$ [g/g]
Cosmogenic background rates [counts/day/kton]		
$^{11}\text{C}$	1860	
$^{10}\text{C}$	35	
Solar neutrino signal rates [counts/day/kton]		
pp $\nu$	1378	
$^7\text{Be}$ $\nu$	517	
pep $\nu$	28	
$^8\text{B}$ $\nu$	4.5	
$^{13}\text{N}/^{15}\text{O}/^{17}\text{F}$ $\nu$	7.5/5.4/0.1	

One of the major concerns in solar neutrino physics is the so called "solar metallicity problem" (SMP), about the content of metals in the core of the Sun [6]. These different possible versions of low Z vs. high Z of the Standard Solar Model affects the neutrino fluxes. An improvement in the accuracy of the determination of the flux for  $^7\text{Be}$  and for  $^8\text{B}$ , could help in solving the SMP.

As shown in the left panel of figure 4 the experimental results are compatible with the predictions for both the low Z and high Z models; this means that it is not possible to definitely solve this ambiguity only by looking at  $^7\text{Be}$  and  $^8\text{B}$  fluxes. A breakthrough would come with the measurement of the CNO neutrino fluxes, as shown in the right panel of figure 4. This graph also indicates that a parallel improvement in the determination of one of the two fluxes, measurable with the JUNO detector, would bring a complementary piece of information, essential to discriminate the ambiguity between high Z models and models, predicting low Z metallicity with modified opacity.

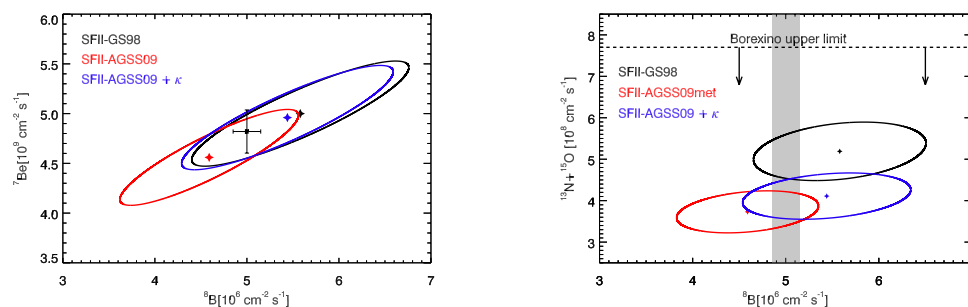


**Figure 4.** Theoretical predictions and experimental results for solar  $\nu$  fluxes. The  $^8\text{B}$  flux is reported on the x-axis; on the vertical axis, instead, one can see the fluxes of  $^7\text{Be}$  (left graph) and of  $^{13}\text{N} + ^{15}\text{O}$ , from CNO cycle, (right graph). The  $1\sigma$  experimental results correspond to black bars in the left graph and to shaded gray vertical band in the right one. The  $1\sigma$  theoretical allowed regions in high Z, low Z and low Z with modified opacity versions of SSM correspond, respectively, to black, red and blue ellipses. Taken from [7].

The possibility of observing  $^8\text{B}$  neutrino is guaranteed in an experiment characterized by an high photon yield, like JUNO, with a relatively low threshold and very good energy resolution. The main problem is due to cosmogenic background of long lived spallation radioisotopes. The most troublesome for the  $\nu_e$  elastic scattering channel are  $^8\text{Li}$ ,  $^{16}\text{N}$  and, in particular the  $^{11}\text{Be}$ , whose spectrum covers almost all the energy regions of interest and decay slowly ( $\gg 1$  s).

Beside the standard  $\nu_e$  elastic scattering, another channel for the  $^8\text{B}$  neutrinos study is the charged current interaction, mainly with  $^{13}\text{C}$  with an energy threshold of 2.2 MeV.

Another open issue in solar neutrino physics is the study of the transition region between the low energy vacuum oscillation and the higher energies, where the MSW mechanism dominates. It is important to test the stability of the LMA oscillation solution, also considering additional contributions to the "standard" oscillation pattern, due, for instance, to Non Standard neutrino Interactions (NSI).

The high statistics and the excellent energy resolution of JUNO could perform a detailed study of the spectrum in the transition region around 3-4 MeV.

#### 4.3. Geoneutrinos

Natural radioactivity, within the Earth, represent a powerful source of heat, influencing the thermal history of our planet. Radiogenic and primordial Earth heat constitute two of the main contributions to the total energy loss of the Earth. Available measurements of temperature gradients in mines gives a total thermal production of  $46 \pm 3$  TW.

Measuring the  $\bar{\nu}_e$ , emitted in the  $^{238}\text{U}$  and  $^{232}\text{Th}$  radioactive decay chains (geoneutrinos), and testing the Th/U rate helps in understanding the abundance of radioactive elements and, therefore, the radiogenic heat contribution and therefore the Earth composition (see for instance [8]).

The potential of JUNO detector for the geoneutrino measurements is due to its depth and radiopurity and, in particular, to its huge size. The main difficulty comes from the presence of a very significant background, with respect to the analyzed signal of  $\bar{\nu}_e$  inverse  $\beta$  decay, due to reactor antineutrinos, as shown in figure 5, where the expected geoneutrino signal is represented in red.

Despite the reactor antineutrinos big contribution, one expects an important geoneutrino measurement at JUNO, which already in the first year of data taking should detect among 300 and 500 events, that is more than the number of geoneutrinos detected by that time by all the other available experiments (KamLAND, Borexino and SNO+).

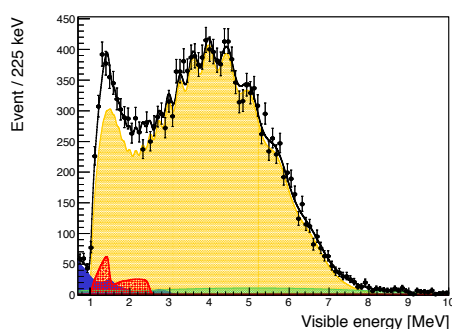


**Figure 5.** Monte Carlo estimate of the prompt IBD candidates for 1 year of measurements, with fixed chondritic Th/U mass ratio. The expected geo- $\nu$  signal is represented in red and other components are: the reactor antineutrinos (orange), main background component,  $^9\text{Li} - ^8\text{He}$  (green), accidental (blue). From [2]

## 5. Conclusion

The Juno detector, with an unprecedented size, PMT coverage, light yield and energy resolution, has a high potentiality in determining the neutrino mass hierarchy, using neutrino oscillations in vacuum. It is rapidly progressing through the design, prototyping and construction phases and besides

its main physics goal, it will also be able to precisely measure the neutrino oscillation parameters below the 1% level, pursuing a rich neutrino physics and astrophysics program. The experiment is scheduled to start data taking in 2021.

## References

1. X. Qian, P. Vogel, *PPNP*, **83**, 1-30 (2015)
2. F. An *et al.* [JUNO Collaboration], *J. Phys. G* **43 no.3**, 030401 (2016)
3. I. Esteban, M.C. Gonzalez-Garcia, M. Maltoni, I. Martinez-Soler, and T. Schwetz 2016, *JHEP* **87**, (2017)
4. S. Choubey, S. T. Petcov and M. Piai, *Phys. Rev. D* **68**, 113006 (2003)
5. F. Di Lodovico, *Advanced Series on Directions in High Energy Physics*, pp 261-297 (2018). doi/10.1142/97898132260980007
6. V. Antonelli, L. Miramonti, C. Pena Garay and A. Serenelli, *Adv. High Energy Phys.* **2013**, 351926 (2013)
7. Serenelli, A. M., talk given at "A special Borexino event - Borexino Mini-Workshop - 2014", Gran Sasso, Sep. 2014; available online from the site <http://borex.lngs.infn.it/>.
8. G. Bellini, A. Ianni, L. Ludhova, F. Mantovani and W. F. McDonough, *Prog. Part. Nucl. Phys.* **73**, 1 (2013)